Delays, Connection Topology, and Synchronization of Coupled Chaotic Maps

Fatihcan M. Atay* and Jürgen Jost†

Max Planck Institute for Mathematics in the Sciences, Leipzig 04103, Germany

Andreas Wende

Department of Computer Science, University of Leipzig, Leipzig 04109, Germany

We consider networks of coupled maps where the connections between units involve time delays. We show that, similar to the undelayed case, the synchronization of the network depends on the connection topology, characterized by the spectrum of the graph Laplacian. Consequently, scale-free and random networks are capable of synchronizing despite the delayed flow of information, whereas regular networks with nearest-neighbor connections and their small-world variants generally exhibit poor synchronization. On the other hand, connection delays can actually be conducive to synchronization, so that it is possible for the delayed system to synchronize where the undelayed system does not. Furthermore, the delays determine the synchronized dynamics, leading to the emergence of a wide range of new collective behavior which the individual units are incapable of producing in isolation.

     PACS numbers: 05.45.Ra, 05.45.Xt, 89.75.–k

Recent years have witnessed a growing interest in the dynamics of interacting units. Particularly, a large number of studies have been devoted to synchronization in a variety of systems (see [1] and the references therein), including the coupled map lattices introduced by Kaneko [2]. Usually, such systems have been investigated under the assumption of a certain regularity in the connection topology, where units are coupled to their nearest neighbors or to all other units. Lately, more general networks with random, small-world, scale-free, and hierarchical architectures have been emphasized as appropriate models of interaction [3–7]. On the other hand, realistic modeling of many large networks with nonlocal interaction inevitably requires connection delays to be taken into account, since they naturally arise as a consequence of finite information transmission and processing speeds among the units. Some numerical studies have regarded synchronization under delays for special cases such as globally coupled logistic maps [8] or carefully chosen delays [9]. In this Letter, we consider synchronization of coupled chaotic maps for general network architectures and connection delays. Because of the presence of the delays, the constituent units are unaware of the present state of the others; so it is not evident *a priori* that such a collection of chaotic units can operate in unison, i.e., synchronize. Based on analytical calculations, we show that this is indeed possible, and in fact may be facilitated by the presence of delays. Moreover, while the connection topology is important for synchronization, the delays have a crucial role in determining the resulting collective dynamics. As a result, the synchronized system can exhibit a plethora of new behavior in the presence of delays. We illustrate the results by numerical simulation of large networks of logistic maps.

We consider a finite connected graph Γ with nodes (vertices) i, writing $i \sim j$ when i and j are neighbors,

that is, connected by an edge, and with the number of neighbors of i denoted by n_i. On Γ, we have a dynamical system with discrete time $t \in \mathbf{Z}$, with the state x_i of i evolving according to

$$x_i(t+1) = f(x_i(t)) + \varepsilon \left[\frac{1}{n_i} \sum_{\substack{j \\ j \sim i}} f(x_j(t-\tau)) - f(x_i(t)) \right].$$
(1)

Here f is a differentiable function mapping some finite interval, say $[0,1]$, to itself, $\varepsilon \in [0,1]$ is the coupling strength, and $\tau \in \mathbf{Z}^+$ is the transmission delay between vertices. A synchronized solution is one where the states of all vertices are identical,

$$x_i(t) = x(t) \quad \text{for all } i.$$
(2)

Thus, $x(t)$ satisfies

$$x(t+1) = (1-\varepsilon)f(x(t)) + \varepsilon f(x(t-\tau)).$$
(3)

In order to investigate the stability of the synchronized solution (see [1] for a description of the stability concept employed here), we consider orthonormal eigenmodes u^k of the graph Laplacian Δ_Γ, defined by $(\Delta_\Gamma v)_i := (1/n_i)\sum_{j \sim i}(v_j - v_i)$, with corresponding eigenvalues $-\lambda_k$. The spectrum of Δ_Γ reflects the underlying connection topology, with the zero eigenvalue λ_0 corresponding to the constant eigenfunction [10]. Since the eigenfunctions yield an L^2 basis for functions on Γ, it suffices to consider perturbations of x of the form

$$x_i(t) = x(t) + \delta\alpha_k(t)u_i^k(t)$$
(4)

for some small δ, and for $k > 0$, that is, nonconstant ones. The solution x is stable against such a perturbation when $\alpha_k(t) \to 0$ for $t \to \infty$. Expanding about $\delta = 0$ yields

$$\alpha_k(t+1) = (1-\varepsilon)f'(x(t))\alpha_k(t)$$
$$+ \varepsilon(1-\lambda_k)f'(x(t-\tau))\alpha_k(t-\tau). \quad (5)$$

The sufficient local stability condition is

$$\lim_{T\to\infty}\frac{1}{T}\log\frac{|\alpha_k(T)|}{|\alpha_k(0)|} < 0. \quad (6)$$

In the case without delay, that is $\tau = 0$, this is rewritten as

$$\lim_{T\to\infty}\frac{1}{T}\log\prod_{t=0}^{T-1}\frac{|\alpha_k(t+1)|}{|\alpha_k(t)|} < 0, \quad (7)$$

and, by (5), becomes

$$\log|1-\varepsilon\lambda_k| + \lim_{T\to\infty}\frac{1}{T}\sum_{t=0}^{T-1}\log|f'(x(t))| < 0, \quad (8)$$

that is

$$|e^\mu(1-\varepsilon\lambda_k)| < 1, \quad (9)$$

where $\mu = \lim_{T\to\infty}\frac{1}{T}\sum_{t=0}^{T-1}\log|f'(x(t))|$ is the Lyapunov exponent of f.

Essentially the same reasoning works for the case of nonzero delay τ. Depending on whether $|\alpha_k(t)|$ is larger than $|\alpha_k(t-\tau)|$ or not, in (7), we either keep the quotient $|\alpha_k(t+1)/\alpha_k(t)|$ or replace it with $|\alpha_k(t+1)/\alpha_k(t-\tau)|$. This reduces the number of factors in (7) by τ, but since we also get correspondingly fewer factors in the term leading to the first term in (8), the left-hand side of (8) is changed by a positive multiplicative factor which does not affect the inequality. The terms get slightly more complicated, as instead of

$$(1-\epsilon\lambda_k)f'(x(t))\alpha_k(t) \quad (10)$$

yielding the two terms in (8), we now have

$$(1-\epsilon)f'(x(t))\alpha_k(t) + \varepsilon(1-\lambda_k)f'(x(t-\tau))\alpha_k(t-\tau)$$
$$(11)$$

from (5). When comparing (10) and (11), we see that in (11) we may get additional partial cancellations due to different signs of $f'(x(t))$ and $f'(x(t-\tau))$ or $\alpha_k(t)$ and $\alpha_k(t-\tau)$, so that the absolute value can be significantly smaller, thereby making the synchronization condition easier to achieve. On the other hand, in a chaotic regime the values of $f'(x(t))$ and $f'(x(t-\tau))$ should be essentially uncorrelated so that we still obtain the Lyapunov exponent μ as the relevant parameter coming from f. A detailed analysis will appear elsewhere, but the foregoing ideas suggest that synchronization in the delayed case is at least not more difficult, but potentially easier [due to cancellations in (11)] to achieve than in the nondelayed one. Moreover, the connection topology, as reflected by the eigenvalues λ_k, still plays an important role in synchronization.

As an application, we take f to be the logistic map

$$f(x) = \rho x(1-x), \quad (12)$$

which possesses a rich dynamical structure depending on

the value of the parameter ρ [12]. Figure 1 shows the synchronization regions in the parameter space for several common network architectures at the value $\rho = 4$ for which f is fully chaotic. The gray-scale encoding represents the degree of synchronization of the network after an initial transient of 10 000 time steps, as measured by the fluctuations $\sigma^2(t) = \sum_{i=1}^{N}(x_i(t) - \bar{x}(t))^2$, where N is the size of the network and $\bar{x}(t) = (1/N)\sum_{i=1}^{N}x_i(t)$. Thus, $\sigma^2(t) \to 0$ as $t \to \infty$ if the system synchronizes. Darker colors in the figure correspond to smaller values of σ^2, with black indicating that $\sigma^2(t) < 10^{-25}$ after the transients. The networks used in the simulations have the same size, $N = 10\,000$, and the same number of average
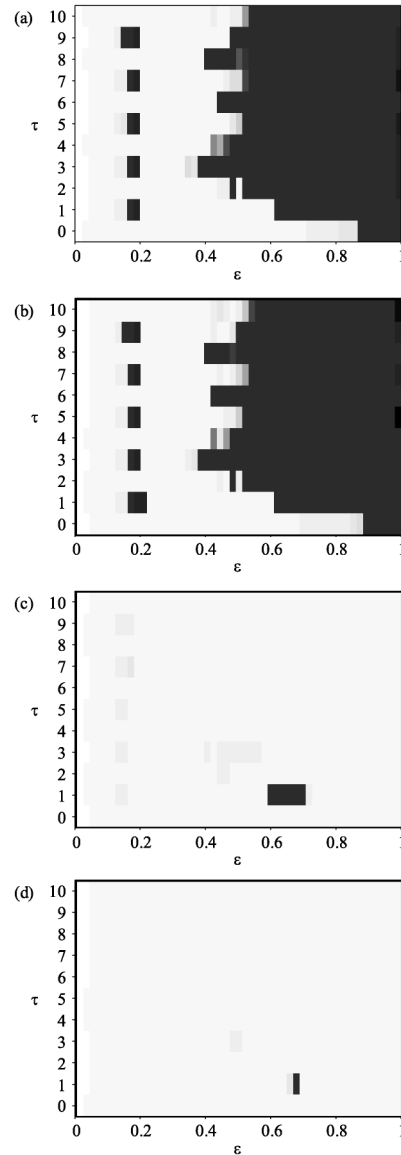

FIG. 1. Synchronization of coupled logistic maps for different values of coupling strength ε and connection delays τ, for the cases of (a) scale-free, (b) random, (c) small-world, and (d) nearest-neighbor coupling. The gray scale encodes the degree of synchronization, with black regions corresponding to complete synchronization.
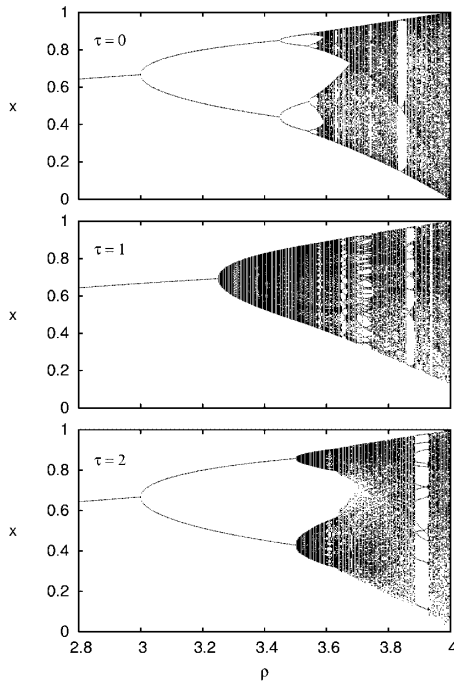
FIG. 2.   The bifurcation diagram of the synchronized solution of coupled logistic maps for several values of τ. At each value of ρ, 200 iterates of (3) are plotted after initial transients. The value of ε is 0.8.

connections, even though the architectures may be different [13]. The effects of the network topology are clearly seen in Fig. 1: Scale-free and random networks can synchronize for a large range of parameters whereas more regular networks with nearest-neighbor and small-world-type coupling do not. In this respect, the similarities between scale-free and random networks [Figs. 1(a) and 1(b)] are noteworthy. A closer inspection reveals some common features for synchronizing networks. For strong coupling (roughly for $\varepsilon > 0.6$), synchronization is achieved regardless of the actual value of the delay, as long as it is positive. For intermediate coupling in the range $0.4 < \varepsilon < 0.6$, the value of the delay becomes decisive for synchronization. In this range, one may also observe long transients, clustering, and on-off intermittency [1], in the gray regions where ε is slightly below the synchronization value. There are also smaller regions of synchronization that exist for weaker coupling ($0.15 < \varepsilon < 0.20$) and only for odd delays. Note that for zero delay synchronization can occur only for a rather limited range ($\varepsilon > 0.85$). Also, the small region of synchronization in Figs. 1(c) and 1(d) occurs for nonzero delay. Therefore, the presence of delays can indeed facilitate synchronization.

While the connection topology is important for the synchronizability of the coupled system, connection delays are significant in determining the resulting synchronized dynamics. In particular, there is an important difference with the undelayed case, for which (3) reduces to

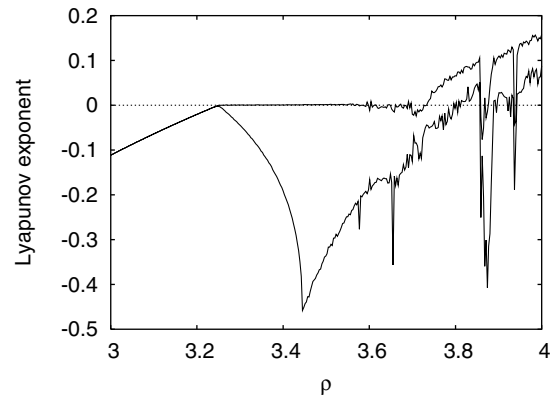$$x(t + 1) = f(x(t)), \tag{13}$$

144101-3

FIG. 3.   The Lyapunov exponents of the synchronized solution for $\tau = 1$ and $\varepsilon = 0.8$.

i.e., when the synchronized system can exhibit nothing different from the exact dynamics of the individual isolated unit. Hence, an important implication of connection delays is the possibility of the emergence of new collective phenomena. Indeed, the solutions of (3) exhibit a much richer range of dynamics when τ is nonzero. Figure 2 shows the bifurcation diagram for several values of τ when f is given by (12). Of course, for $\tau = 0$ the familiar bifurcation diagram of the logistic map is obtained, displaying the period-doubling route to chaos. By contrast, when $\tau > 0$, Neimark-Sacker–type bifurcations [12] are prevalent, immediately resulting in high-period solutions followed by more complex behavior. Other values of odd and even delays result in pictures similar to the cases $\tau = 1$ and $\tau = 2$, respectively. Since Neimark-Sacker bifurcations cannot arise in one-dimensional maps, the difference with the undelayed case is fundamental. Similarly, a consideration of the Lyapunov exponents shows that the character of the chaotic attractor is also different. For instance, as seen in Fig. 3, the synchronized system can have two positive Lyapunov exponents when connection delays are present, thus exhibiting hyperchaos.
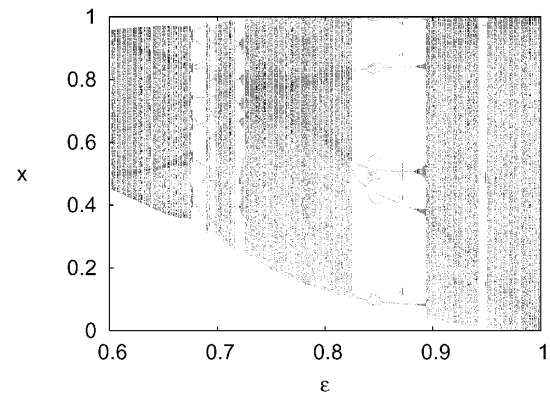

FIG. 4.   The synchronized solution at different coupling strengths for $\tau = 1$ and $\rho = 4$. At each value of ε, 300 iterates of (3) are plotted after initial transients.
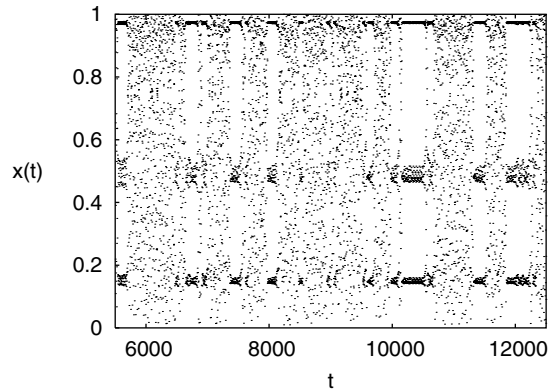
FIG. 5. Intermittent behavior of synchronized logistic maps for $\rho = 4$, $\varepsilon = 0.95$, and $\tau = 1$.

Connection delays make the coupling strength ε an important factor in the dynamics of the synchronized solutions. To demonstrate, we take the logistic map (12) with $\rho = 4$, for which it has a chaotic attractor. Thus, (3) is chaotic for all ε when $\tau = 0$. By contrast, when $\tau = 1$, the attracting solutions of (3) display a wider variety depending on the value of ε, as depicted in Fig. 4. Chaos is interrupted by windows of stable periodic solutions, for instance, near $\varepsilon = 0.68$ and $\varepsilon = 0.71$. There is a large window of period-5 solutions for $0.82 < \varepsilon < 0.89$, which also contain other stable solutions of higher periods for certain ε in this range. A periodic attractor of period 3 exists near $\varepsilon = 0.945$, which transforms to intermittent behavior at $\varepsilon = 0.95$, shown in Fig. 5. All these dynamics are exhibited by the coupled system (1), since Fig. 1 implies that for these parameter values the system is synchronized (provided it has an appropriate connection topology), so the collective behavior is described by (3). Clearly, delays can make the dynamics of the synchronized system quite sensitive to the coupling strength, a feature that is absent in undelayed networks.

Networks with connection delays arise naturally in many areas of science, including biology, population dynamics, neuroscience, economics, and so on. In neural systems, for instance, delays result from, e.g., finite axonal transmission speeds [14]. Such networks lack an intrinsic notion of simultaneity since the present state of the system is inaccessible to the constituent units. These networks are nevertheless capable of operating in synchrony, even when complex units and significantly large delays are involved, as our findings indicate. In fact, networks with delays can actually synchronize more easily. This synchronizability property is especially relevant for neural networks, circumventing the difficulties in establishing a concept of collective or simultaneous information processing in the presence of delayed information transmission [15]. Furthermore, the delays shape the dynamics of the synchronized system, leading to the emergence of a variety of new dynamics which the individual units are not capable of producing [16]. The observation that a wide range of different behavior can be accessed by varying the coupling strength has important implications for neural networks, where synaptic coupling strengths can change through learning. This interesting connection provides additional motivation for investigating the role of delays in complex adaptive systems.

---

[1] A. Pikovsky, M. Rosenblum, and J. Kurths, *Synchronization–A Universal Concept in Nonlinear Science* (Cambridge University Press, Cambridge, England, 2001).
[2] K. Kaneko, Prog. Theor. Phys. **72**, 480 (1984).
[3] P. M. Gade, H. A. Cerdeira, and R. Ramaswamy, Phys. Rev. E **52**, 2478 (1995).
[4] P. M. Gade, Phys. Rev. E **54**, 64 (1996).
[5] D. J. Watts and S. H. Strogatz, Nature (London) **393**, 440 (1998).
[6] A. L. Barabasi and R. A. Albert, Science **286**, 509 (1999).
[7] M. G. Cosenza and K. Tucci, Phys. Rev. E **64**, 026208 (2001).
[8] Y. Jiang, Phys. Lett. A **267**, 342 (2000).
[9] C. Masoller, A. C. Marti, and D. H. Zanette, Physica (Amsterdam) **325A**, 186 (2003).
[10] We follow here the conventions of [11] where also further references can be found. The eigenvalues are labeled in increasing order, the smallest one being the trivial eigenvalue $\lambda_0 = 0$.
[11] J. Jost and M. P. Joy, Phys. Rev. E **65**, 016201 (2002).
[12] S. N. Elaydi, *Discrete Chaos* (Chapman & Hall/CRC, Boca Raton, FL, 2000).
[13] The regular networks used in simulations have circular arrangement with each node coupled to its nearest k neighbors, where k is an even integer. Such networks are known to synchronize only for sufficiently small system sizes in the undelayed case [11]. Small-world architecture is obtained by replacing randomly selected edges with long-range connections [5]. Scale-free networks are constructed using the algorithm of Barabasi and Albert [6], starting with ten isolated nodes and adding one node and ten links at each step. Each network consists of 10 000 nodes and about 10^5 links.
[14] F. M. Atay and A. Hutt, Max Planck Institute for Mathematics in the Sciences Preprint Series No. 54 (2003).
[15] See also U. Ernst, K. Pawelzik, and T. Geisel, Phys. Rev. Lett. **74**, 1570 (1995); W. Gerstner, Phys. Rev. Lett. **76**, 1755 (1996), in the context of coupled integrate-and-fire neurons.
[16] For further discussion along this line, see F. M. Atay and J. Jost, Max Planck Institute for Mathematics in the Sciences, Preprint Series No. 102 (2003); arXiv:nlin.AO/0312026.